STRUCTURAL SCIENCE
CRYSTAL ENGINEERING
MATERIALS

ISSN: 2052-5206
journals.iucr.org/b

Molecular structures of two copper complexes with the pharmaceuticals norfloxacin and tinidazole, when powder X-ray diffraction assists multi-domain single-crystal X-ray diffraction

Gloria Elena Tobón Zapata, Dina Marcela Martínez Carmona, Gustavo Alberto Echeverría and Oscar Enrique Piro

Acta Cryst. (2022). B**78**, 490–498

Acta Cryst B STRUCTURAL SCIENCE CRYSTAL ENGINEERING MATERIALS

ISSN 2052-5206

Molecular structures of two copper complexes with the pharmaceuticals norfloxacin and tinidazole, when powder X-ray diffraction assists multi-domain single-crystal X-ray diffraction

Gloria Elena Tobón Zapata,[a] Dina Marcela Martínez Carmona,[a] Gustavo Alberto Echeverría[b] and Oscar Enrique Piro[b]*

[a]Departamento de Farmacia, Facultad de Ciencias Farmacéuticas y Alimentarias, Universidad de Antioquía, AA 1226, Colombia, and [b]Departamento de Física, Facultad de Ciencias Exactas, Universidad Nacional de La Plata and IFLP (CONICET), C.C. 67, 1900 La Plata, Argentina. *Correspondence e-mail: piro@fisica.unlp.edu.ar

Received 9 January 2022
Accepted 5 April 2022

Edited by K. E. Knope, Georgetown University, USA

Keywords: copper(II) complexes of norfloxacin and tinidazole; X-ray crystal structures; PXRD-assisted SCXRD; vibrational IR spectra; thermal decomposition.

CCDC references: 900244; 2082848

Supporting information: this article has supporting information at journals.iucr.org/b

The crystal structures of bis[1-ethyl-6-fluoro-4-oxo-7-(piperazin-1-ium-4-yl)-1,4-dihydroquinoline-3-carboxylato]copper(II) sulfate heptahydrate, $[Cu(C_{16}H_{18}FN_3O_3)_2]SO_4{\cdot}7H_2O$ or $[Cu(nor)_2]SO_4{\cdot}7H_2O$ (nor is norfloxacin), and bis{1-[2-(ethylsulfonyl)ethyl]-2-methyl-5-nitroimide}dinitratocopper(II), $[Cu(NO_3)_2(C_8H_{13}N_3O_4S)_2]$ or $[Cu(NO_3)_2(tnz)_2]$ (tnz is tinidazole), were solved by X-ray diffraction. Both complexes crystallize in the space group $P2_1/c$, with $Z = 4$ (for nor) and $Z = 2$ (for ntz) molecules per unit cell. In $[Cu(nor)_2]SO_4{\cdot}7H_2O$, the Cu^{II} ion is at the centre of a square-planar environment, *trans* coordinated to two independent norfloxacin molecules in the zwitterionic form acting as bidentate ligands through one of the carboxyl (cbx) and the carbonyl (cb) O atoms. The solid is further stabilized by an extensive network of N—H···O(sulfate), N—H···O(cbx), N—H···O*W*, O*W*—H···O(sulfate) and O*W*—H···O*W* hydrogen bonds. The $[Cu(NO_3)_2(tnz)_2]$ complex is centrosymmetric, with the Cu^{II} ion in a square planar environment, coordinated to a tinidazole molecule acting as a monodentate ligand through its imidazole N atom and to one nitrate O atom. The vibrational FT–IR absorption spectra and thermal behaviour of the complexes were also studied and are briefly discussed based on the crystal structures.

1. Introduction

Norfloxacin (nor; see Scheme 1), belonging to the quinolone family, is a synthetic antibacterial agent. It acts by inhibiting bacterial DNA replication and is widely employed in the treatment of diverse infections (Sekhon & Gandhi, 2001). The binding of metallic ions has been shown to increase the activity of some antibiotics and substantial improvement in the pharmacological action of fluoroquinolones complexed with copper has been reported (Turel, 2002; Efthimiadou *et al.*, 2007). Furthermore, the interaction of various metal ions with quinolones has been studied intensely (Turel, 2002) and several copper(II)–quinolone complexes have been reported in the literature (Efthimiadou *et al.*, 2007; Wang *et al.*, 2003; Wallis *et al.*, 1996; Refat, 2007). On the other hand, compounds that have an imidazole ring in the molecular structure are recognized for their antifungal action and sedative or anti-microbial (nitroimidazoles) properties. Among these aggregates is 1-[2-(ethylsulfonyl)ethyl]-2-methyl-5-nitroimidazole (tinidazole, tnz; Scheme 1) (Sánchez-Guadarrama *et al.*, 2009). In human medicine, there are reports of anti-inflammatory, anti-ulcer, antiseizure, anti-emetic, antitumour and anti-

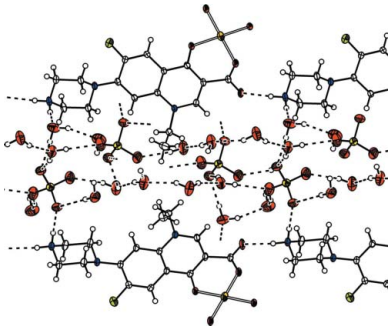

Table 1
Crystal data and structure refinement results for complexes $[Cu(nor)_2]SO_4{\cdot}7H_2O$ and $[Cu(NO_3)_2(tnz)_2]$.

Complex	$[Cu(nor)_2]SO_4{\cdot}7H_2O$	$[Cu(NO_3)_2(tnz)_2]$
Chemical formula	$C_{32}H_{50}CuF_2N_6O_{17}S$	$C_{16}H_{26}CuN_8O_{14}S_2$
Formula weight	924.38	682.11
Temperature (K)	295 (2)	296 (2)
Wavelength (Å)	1.54184	0.71073
Crystal system	Monoclinic	Monoclinic
Space group	$P2_1/c$	$P2_1/c$
Unit-cell dimensions		
a (Å)	10.4613 (3)	7.3063 (3)
b (Å)	31.2244 (8)	10.8907 (5)
c (Å)	12.2241 (3)	16.4396 (5)
β (°)	104.450 (3)	90.670 (3)
Volume (Å^3)	3866.7 (2)	1308.02 (9)
Z	4	2
Density (calculated, Mg m^{-3})	1.588	1.732
Absorption coefficient (mm^{-1})	2.126	1.079
$F(000)$	1932	702
Crystal colour	Blue	Blue
Crystal size (mm)	0.43 × 0.17 × 0.03	0.255 × 0.179 × 0.042
θ range (°) for data collection	3.99–70.97	3.105–28.814
No. of reflections collected	15203	5901
No. of independent reflections	7439 (R_{int} = 0.0347)	2850 (R_{int} = 0.0350)
No. of observed reflections [$I > 2\sigma(I)$]	5339	2257
Completeness (%)	99.8 (to θ = 70.97°)	99.9 (to θ = 25.242°)
Refinement method	Full-matrix least-squares on F^2	Full-matrix least-squares on F^2
No. of data, restraints, parameters	7439, 19, 571	2850, 0, 189
Goodness-of-fit on F^2	1.005	1.058
Final R indices[a] [$I > 2\sigma(I)$]	$R1$ = 0.0472, wR_2 = 0.1220	R_1 = 0.0431, wR_2 = 0.0935
R indices (all data)	R_1 = 0.0688, $wR2$ = 0.1421	$R1$ = 0.0605, $wR2$ = 0.1033
Largest difference peak, hole (e Å^{-3})	0.532, −0.387	0.496, −0.355

Note: (*a*) $R_1 = \Sigma||F_o| - |F_c||/\Sigma|F_o|$, $wR_2 = [\Sigma w(|F_o|^2 - |F_c|^2)^2/\Sigma w(|F_o|^2)^2]^{1/2}$. Computer programs: *CrysAlis PRO* (Agilent, 2011, Rigaku OD, 2015), *SHELXT* (Sheldrick, 2015*a*), *SHELXL2014* (Sheldrick, 2015*b*) and *ORTEP for Windows* (Farrugia, 2012).

microbial activity of these compounds. In general, the biological action of the ligand is enhanced through the formation of complexes with metal ions that possess similar activity, hence the importance of the coordination compounds of imidazole with transition metals, copper in the present study, which has antimicrobial activity (Roat, 2007; Ali *et al.*, 2017).

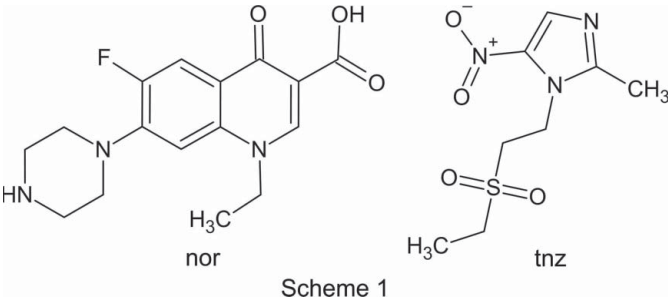

Scheme 1

2. Materials and methods

2.1. Synthesis

2.1.1. $[Cu(nor)_2]SO_4{\cdot}7H_2O$. Norfloxacin (nor), provided by Provefarma, was characterized as a dihydrate (Chongcharoen *et al.*, 2008) by IR, powder X-ray diffraction (PXRD), thermogravimetric analysis (TGA) and differential thermal analysis (DTA) techniques. The copper-containing reactant $Cu_2SO_4{\cdot}5H_2O$ and methanol solvent were of Merck reagent grade and were employed without further purification. The $[Cu(nor)_2]SO_4{\cdot}7H_2O$ complex was obtained following the procedure reported by Refat (2007). 1 mmol of $CuSO_4{\cdot}6H_2O$ was added to 2 mmoles of norfloxacin dihydrate dissolved in a methanol–water mixture (1:1 *v*/*v*), under continuous stirring at room temperature for a period of 8 h. After a further 20 h, the deposited solid was filtered off and washed with methanol. The resulting product was dissolved in methanol and kept at 20 °C for three weeks to afford the formation, by slow solvent evaporation, of blue single crystals adequate for structural X-ray diffraction work. The crystalline sample was characterized by IR, PXRD and TGA–DTA techniques. The reaction yield was 54%; copper content (%): 6.68 (found), 6.87 (calculated).

2.1.2. $[Cu(NO_3)_2(tnz)_2]$. Tinidazole (tnz), provided by Laproff Laboratories, was characterized as described above for norfloxacin. The copper-containing reactant $Cu(NO_3)_2{\cdot}3H_2O$ and ethanol solvent were of Merck reagent grade and were employed without further purification. The $[Cu(NO_3)_2(tnz)_2]$ complex was obtained following the procedure reported by Alfaro-Fuentes *et al.* (2014) by adding the respective salt dissolved in ethanol and then mixing with a hot ethanol solution of tinidazole. The mixture was refluxed for 4 h, followed by rapid cooling in an ice bath. The precipitate was filtered off and blue crystals were obtained from the mother solution. The solid sample was characterized by IR, PXRD, TGA and DSC techniques. The reaction yield was 71%; copper content (%): 9.00 (found), 9.32 (calculated).

2.2. Single-crystal X-ray diffraction

Crystal data, data collection and structure refinement details are summarized in Table 1. The measurements were performed on a Rigaku Oxford Gemini Eos CCD diffractometer with graphite-monochromated Cu $K\alpha$ (λ = 1.54178 Å) radiation for $[Cu(nor)_2]SO_4{\cdot}7H_2O$ and Mo $K\alpha$ (λ = 0.71073 Å) radiation for $[Cu(NO_3)_2(tnz)_2]$. X-ray diffraction intensities were collected (ω scans with θ- and κ-offsets), integrated and scaled with the *CrysAlis PRO* (Agilent, 2011; Rigaku OD, 2015) suite of programs. The unit-cell parameters were obtained by least-squares refinement (based on the angular settings for all the collected reflections with intensities greater than seven times the standard deviation of the measurement errors) using *CrysAlis PRO*. Data were corrected empirically for absorption employing the multi-scan method implemented in *CrysAlis PRO*.

2.2.1. $[Cu(nor)_2]SO_4{\cdot}7H_2O$. The structure was solved by intrinsic phasing with *SHELXT* (Sheldrick, 2015*a*) and the molecular models refined with *SHELXL* (Sheldrick, 2015*b*) of the *SHELX* (Sheldrick, 2008) suite of programs. All H atoms of the norfloxacin molecules, including those of $-NH_2^+$ revealing the zwitterionic form of the ligand, were found in a difference Fourier map. However, they were positioned at their expected geometrical locations and refined with the riding model. The methyl H-atom positions were optimized by treating them as rigid groups, which were allowed to rotate during the refinement around the corresponding C—C bonds so as to maximize the sum of the residual electron densities at the calculated positions. As a result, both CH_3 groups converged to staggered conformations. A final difference Fourier map, phased on the complete complex, the sulfate anion and the water O atoms, showed all but one (O7*W*) water H atom. These H atoms were refined at their found positions with isotropic displacement parameters equal to 1.5 times the equivalent isotropic displacement parameter of the corresponding water O atom and with O*W*—H and H···H distances restrained to target values of 0.86 (1) and 1.36 (1) Å, respectively.

2.2.2. $[Cu(NO_3)_2(tnz)_2]$. The samples were composed of many single-crystal domains displaying complex optical behaviour when examined under polarized light on a microscope. The first crystals selected showed the X-ray diffraction pattern due to the superposition of the individual signature of several single-crystal domains (in a number larger than, at least, four) having no evident twin laws relating them to one another. This made it difficult to find, by the standard search programs of single-crystal diffractometers, the unit-cell constants of the dominant single-crystal contributors. Obviously, the problem does not arise in the X-ray diffraction pattern of the powdered sample (PXRD), which afforded the determination of unit-cell constants and even the correct space group (Table 2). We then constrained the unit-cell search to look for the unit-cell parameters provided by the PXRD study to unravel up to four contributing domains in the complex diffraction pattern of a multi-single-crystal sample. The structure yielded easily to the intrinsic phasing method when applied to the perturbed X-ray diffraction pattern of the main domain contributor (about 30% scattering power). However, as expected, the data and the refinement that ensued showed anomalies reflecting the superposition of reflections due to the other domains which could not be handled properly with standard de-twinning procedures. The anomalies included relatively large R_{int} and R_σ values (0.121 and 0.125, respectively), systematically much larger values of F_o^2 compared with F_c^2 in the list of most disagreeable reflections, and a large agreement R_1 value (about 0.1) and maximum residual electron density ($\Delta\rho$ = 1.8 e Å^{-3}). We then made an extensive search for and finally found a nearly mono-domain crystal and, as expected, the quality of the data and refinement improved substantially. In fact, now R_{int} = 0.035 and R_σ = 0.053, and the refinement of the initial molecular model against the new untwinned data set converged smoothly to R_1 = 0.0432, the $\Delta\rho$ value dropped to 0.5 e Å^{-3} and the sign of $F_o^2 - F_c^2$ was more evenly distributed. The H atoms were refined as described for those of the norfloxacin ligands in $[Cu(nor)_2]SO_4{\cdot}7H_2O$.

Table 2
Powder diffraction data for $[Cu(NO_3)_2(tnz)_2]$.

Molecular weight (g mol^{-1})	682.11
Crystal system	Monoclinic
Space group	$P2_1/c$
a (Å)	7.3116 (4)
b (Å)	10.8923 (4)
c (Å)	16.4498 (5)
β (°)	90.660 (3)
V (Å^3)	1310.0 (2)
Z	2
D_{calc} (Mg m^{-3})	1.73

2.3. Powder X-ray diffraction (PXRD) data

The PXRD pattern of $[Cu(NO_3)_2(tnz)_2]$ was obtained with a PANalytical Empyrean diffractometer, using Cu $K\alpha$ radiation (λ = 1.541874 Å) from an X-ray tube operated at 45 kV and 40 mA. The X-ray diffraction pattern was collected in the $5 \leq 2\theta \leq 50°$ range, with a 0.02° step width and a 0.5 s counting time per step employing Bragg–Brentano θ–θ geometry, a two-dimensional (2D) solid-state hybrid PIXcel detector and an Ni-filtered exit beam.

The indexing of the X-ray pattern was achieved with *ITO* (Visser, 1969), *TREOR* (Werner *et al.*, 1985) and *DICVOL* (Boultif & Louër, 1991) interfaced from the *CRYSFIRE* suite of programs (Shirley, 2002). The space group was confirmed and the unit-cell parameters refined with *CHEKCELL* (Laugier & Bochu, 2000) and the results are shown in Table 2.

2.4. IR absorption spectra

The IR spectra of both complexes as KBr mulls were collected on an FT–IR PerkinElmer spectrophotometer (Spectrum Bx) in the 4000–400 cm^{-1} frequency range at a resolution of 4 cm^{-1}.

2.5. Thermal analysis

Differential thermal (DT) and thermogravimetric (TG) analyses were performed in the 20–800 °C temperature range for $[Cu(nor)_2]SO_4{\cdot}7H_2O$ with a Shimadzu DTA-50H and TGA-50 units at a heating rate of 5 °C min^{-1} and a nitrogen flow of 50 ml min^{-1}.

A DSC and TGA thermal study of $[Cu(NO_3)_2(tnz)_2]$ was performed with a DSC Netzsch (200 PC-phox) instrument in the 25–450 °C interval at a rate of 10 °C min^{-1}, employing as a sample holder an aluminium crucible kept under a nitrogen atmosphere.

3. Results and discussion

3.1. Crystallographic structural results

3.1.1. $[Cu(nor)_2]SO_4{\cdot}7H_2O$. Fig. 1 is an *ORTEP-3* (Farrugia, 2012) view of the $[Cu(nor)_2]^{2+}$ complex in the $[Cu(nor)_2]SO_4{\cdot}7H_2O$ crystal. The corresponding bond lengths and angles around copper are listed in Table 3. The complex is closely related to the centrosymmetric counterpart found in the perchlorate anhydrous salt (Xie *et al.*, 2004). Excluding the norfloxacin methyl groups and the terminal heterocycles, the complex in the sulfate heptahydrate salt is nearly planar. The Cu^{II} ion is at the centre of a nearly square-planar environment, *trans*-coordinated by two norfloxacin groups acting as bidentate ligands through one of their carboxyl (cbx) and the carbonyl (cb) O atoms [Cu—O(cbx) = 1.899 (2) and 1.900 (2) Å, and Cu—O(cb) = 1.929 (2) and 1.931 (2) Å]. The *trans*-O(cbx)—Cu—O(cbx) and O(cb)—Cu—O(cb) angles are 178.3 (1) and 178.69 (9)°, and the *cis*-O(cbx)—Cu—O(cb) angles are in the range 86.01 (8)–93.82 (2)°.

As expected from the extended π-bond delocalization, the parent 4-oxo-1,4-dihydroquinolone skeleton of both norfloxacin ligands are planar (r.m.s. deviation of the atoms from the best least-squares plane of 0.055 and 0.065 Å). They are nearly coplanar with each other [angled at 6.89 (7)°] and with the CuO_4 core plane [angles of 11.3 (1) and 7.4 (1)°]. The ligands show a zwitterionic form with a negatively charged carboxylic $-COO^-$ group at one molecular end and a positively charged $>NH_2^+$ group on the terminal heterocycle ring at the other end. The zwitterionic form of norfloxacin both as an anhydrate (Barbas *et al.*, 2007) and as hydrates (Roy *et al.*, 2008), as well as as a ligand in binary and tertiary complexes of Cu^{II}, have been reported in the literature (Ruíz *et al.*, 2007).

Table 3
Bond lengths (Å) and angles (°) around copper(II) in $[Cu(nor)_2]SO_4{\cdot}7H_2O$.

Cu—O11	1.900 (2)	O21—Cu—O11	178.25 (9)
Cu—O13	1.929 (2)	O21—Cu—O13	86.49 (8)
Cu—O21	1.898 (2)	O11—Cu—O13	93.83 (8)
Cu—O23	1.931 (2)	O21—Cu—O23	93.71 (8)
		O11—Cu—O23	86.01 (8)
		O13—Cu—O23	178.69 (9)

The sulfate heptahydrate salt of the Cu^{II}–norfloxacin complex dealt with here was described previously as an octahedral $Cu(nor)_2(H_2O)_2$ complex in the $[Cu(nor)_2(H_2O)_2]SO_4{\cdot}5H_2O$ salt (Refat, 2007). Our present crystallographic study shows that none of the seven water molecules coordinates the metal and therefore the substance should be correctly described as $[Cu(nor)_2]SO_4{\cdot}7H_2O$.

The crystal is further stabilized by an extended and complex network of N—H···O(sulfate), N—H···O(cbx), N—H···O*W*, O*W*—H···O(sulf) and O*W*—H···O*W* hydrogen bonds. The crystal packing can be described as electrically charged layers parallel to the crystal (010) plane of $[Cu(nor)_2]^{2+}$ complexes intercalated by layers of hydrated sulfate counter-anions (see Fig. 2). Neighbouring complexes in a layer are related by $\pm$(**a** + **c**) unit-cell translations and are linked to each other through two $>NH_2^+\cdots$O(cbx) hydrogen bonds involving one H atom of the protonated $>NH_2^+$ piperazine group and the unbonded-

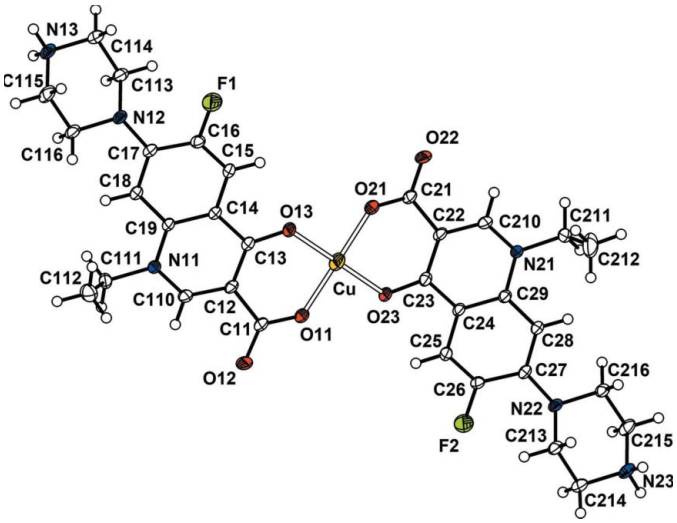

Figure 1
View of the copper–norfloxacin complex in $[Cu(nor)_2]SO_4{\cdot}7H_2O$, showing the labelling of the non-H atoms and their displacement ellipsoids at the 30% probability level. Metal–ligand bonds are indicated by open lines.

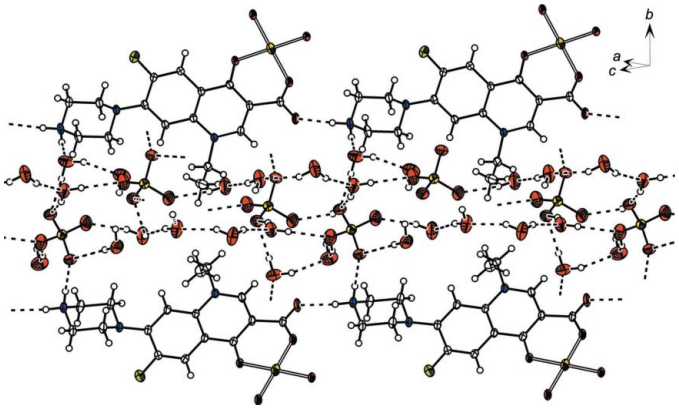

Figure 2
View down the $[\bar{1}01]$ direction of $[Cu(nor)_2]SO_4{\cdot}7H_2O$, showing the layered arrangement parallel to the (010) plane of intercalated slabs of $[Cu(nor)_2]^{2+}$ complexes and hydrated SO_4^{2-} ions, and the hydrogen-bonding network for H···A < 2 Å. Layers of the same kind are symmetry-related through a twofold screw axis along the unique *b* axis of space group $P2_1/c$.

to-copper carboxylate O atom [N···O(cbx) = 2.706 (3) and 2.705 (3) Å, and N—H···O(cbx) = 172 and 166°]. This gives rise to a chain structure that extends along the crystal [101] direction. Neighbouring chains are stacked along [$\bar{1}$01] in a canted fashion. Besides the strong interlayer electrostatic attraction, a layer of complexes binds adjacent layers of hydrated SO_4^{2-} ions through $>NH_2^+\cdots$O(sulf) hydrogen bonding on one layer side and by $>NH_2^+\cdots OW$ hydrogen bonding on the other side, involving the other H atom of the $>NH_2^+$ group [N···O(sulf) = 2.714 (4) Å, N···O*W* = 2.665 (4) Å, N—H···O(sulf) = 178° and N—H···O*W* = 165°]. Detailed hydrogen-bond distances and angles are provided as supporting information (Table S9).

3.1.2. $[Cu(NO_3)_2(tnz)_2]$. A drawing of the $[Cu(NO_3)_2(tnz)_2]$ complex is shown in Fig. 3 and bond lengths and angles around the Cu^{II} ion are given in Table 4. The metal atom is located on a crystallographic inversion centre in a nearly square planar environment. It is coordinated to a tnz molecule acting as a monodentate ligand through its imidazole N atom [Cu—N = 1.990 (2) Å] and to one nitrate O atom [Cu—O = 2.053 (2) Å], nearly along their respective electron lone-pair orbital lobes. The N—Cu—O bond angle is 87.65 (9)°. The NO_3^- molecular plane is oriented such that the other nitrate O atom caps the copper metal at a long Cu···O distance of 2.445 (2) Å and a tilt angle of 55.5 (1)° with respect to the coordination plane. The tnz imidazole ring subtends a dihedral angle of 40.6 (1)° with the coordination plane. Because of the extended π-bonding delocalization throughout the imidazole skeleton, the NO_2 group is nearly coplanar with the heterocyclic ring [angled at 10.8 (1)°].

The Cu—N(tnz) coordination distances and bond lengths and angles in the ligand agree with the corresponding geometrical data reported for the related $Cu(tnz)Cl_2$ complex (Alfaro-Fuentes *et al.*, 2014). The ligand metric of $[Cu(NO_3)_2(tnz)_2]$ also agrees with corresponding values observed for the uncoordinated organic molecule (Chasseaud *et al.*, 1984), but as expected shows in all comparisons appreciable variations in the conformation of the tnz $-(CH_2)_2-SO_2-CH_2-CH_3$ pendant arm. As for $[Cu(nor)_2]SO_4\cdot 7H_2O$, the structural results for

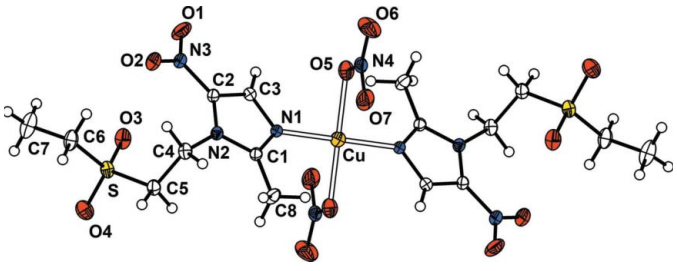

Figure 3
View of the $[Cu(NO_3)_2(tnz)_2]$ centrosymmetric complex, showing the labelling of the non-H atoms and their displacement ellipsoids at the 30% probability level. The unlabelled half of the molecule is obtained from the labelled one through a crystallographic inversion centre at the copper location. The solid shows weak and bent intra- and intermolecular C—H···O hydrogen bonds (H···O > 2.25 Å and C—H···O < 138°). These are detailed in Table S10 of the supporting information.

Table 4
Bond lengths (Å) and angles (°) around copper(II) in centrosymmetric $[Cu(NO_3)_2(tnz)_2]$.

Cu—N1	1.990 (2)	Cu—O5	2.053 (2)
N1—Cu—O5	87.65 (9)		

$[Cu(NO_3)_2(tnz)_2]$ point to a mainly $d_{x^2-y^2}$ orbital for the copper unpaired electron (or hole) ground state.

Upon coordination to the copper ion, there are significant changes in the NO_3^- molecular structure, with the longer N—O bond length of 1.273 (3) Å for the coordinated-to-copper O atom, N—O = 1.229 (4) Å for the capping O atom and N—O = 1.205 (3) Å for the uncoordinated nitrate O atom.

3.2. Powder X-ray diffraction (PXRD) results

Fig. 4 shows a comparison of the PXRD pattern for $[Cu(NO_3)_2(tnz)_2]$ with the calculated one (Yvon *et al.*, 1977) derived from the solid-state molecular structure determined by single-crystal X-ray diffraction. The very good agreement observed between the experimental and theoretical X-ray diffraction patterns shows that the material in its usual polycrystalline aggregation state has the same crystal structure as its single-crystal counterpart without a significant contribution of impurities, hence serving as a useful reference to quickly confirm the identity and purity of any powdered $[Cu(NO_3)_2(tnz)_2]$ pharmaceutical sample. Diagnostic powder diffraction peaks were observed at unique 2θ values (in °) of 9.76, 17.15, 20.34, 23.05, 25.11, 26.23, 27.94, 31.05, 34.82 and 41.33, with an estimated uncertainty of ±0.03°.

3.3. IR spectra

3.3.1. $[Cu(nor)_2]SO_4\cdot 7H_2O$. The vibration IR spectrum (see Fig. 5) agrees with the IR data for the complex reported

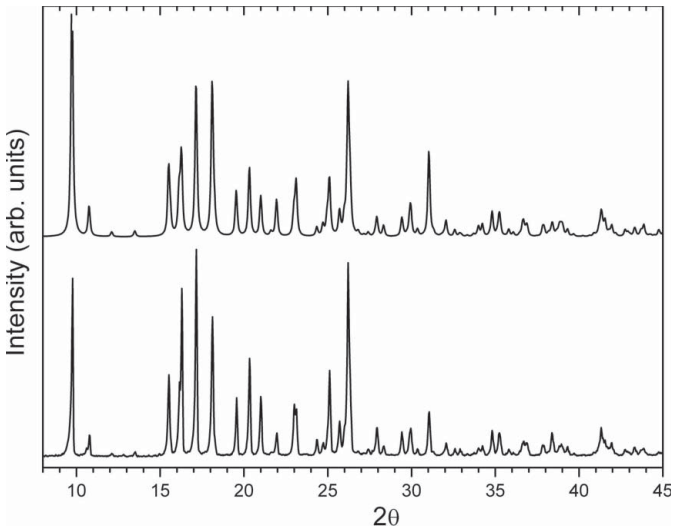

Figure 4
(Lower trace) Experimental powder X-ray diffraction (PXRD) pattern of $[Cu(NO_3)_2(tnz)_2]$ collected with Cu $K\alpha$ radiation. (Upper trace) PXRD pattern calculated from the solid-state molecular structure of $[Cu(NO_3)_2(tnz)_2]$ determined by single-crystal X-ray diffraction methods.

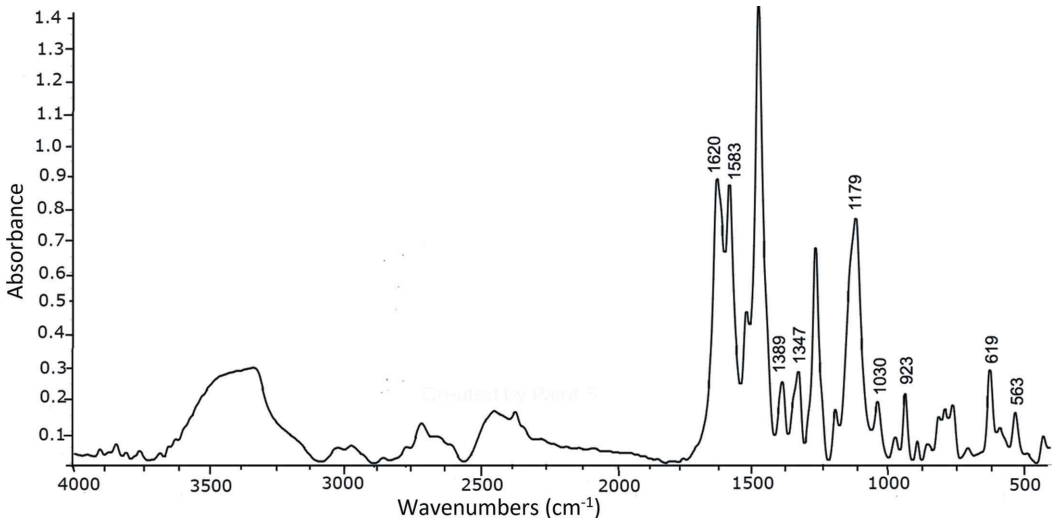

Figure 5
IR absorbance spectrum of solid-state $[Cu(nor)_2]SO_4{\cdot}7H_2O$.

previously (Refat, 2007). It features broad and split bands in the 3600–2300 cm^{-1} spectral region. The intense and broad band between 3600 and 3200 cm^{-1} is mainly due to unresolved absorptions of perturbed asymmetric and symmetric O—H stretching mode of hydrogen-bonded crystallization water molecules. The corresponding absorptions due to water bending modes are included in the band centred at 1583 cm^{-1} and hindered water librational modes are expected below 600 cm^{-1}. The broad and split bands in the 3200–2300 cm^{-1} region include the absorption due to the ν_{asym}(N—H) and ν_{sym}(N—H) stretching modes of norfloxacin $>NH_2^+$ groups, also subjected to perturbing effects of intermolecular N—H···O and N—H···S hydrogen bonds (see Table S9 in the supporting information).

The absence of the absorption due to the ν(C═O) stretch of the carboxylic acid group –(C═O)OH should be noted, which is present at 1730 cm^{-1} in the spectrum of the free ligand. Instead, the copper complex of norfloxacin shows two bands at 1620 and 1389 cm^{-1} which can be respectively assigned to the carboxyl ν(C═O) and ν(C—O) stretching modes of one norfloxacin ligand, while the absorptions due to the carboxyl counterpart of the other, crystallographically different, norfloxacin ligand can be identified with the bands observed at 1583 and 1347 cm^{-1}. This is the spectroscopic signature of the –(C═O)OCu bonding of a COO^- group to the Cu^{II} ion, as disclosed by the X-ray structure of $[Cu(nor)_2]SO_4{\cdot}7H_2O$ presented here.

The two strong absorption bands with maxima at 1179 and 1030 cm^{-1}, and the bands observed at 923 and 619 cm^{-1} are attributed to sulfate vibration modes. The Cu—O stretching vibration is assigned to a medium–weak band at 563 cm^{-1} (Refat, 2007; Ruíz *et al.*, 2007).

3.3.2. $[Cu(NO_3)_2(tnz)_2]$. The IR spectrum of $[Cu(NO_3)_2(tnz)_2]$ is shown in Fig. 6. The frequencies of some of the

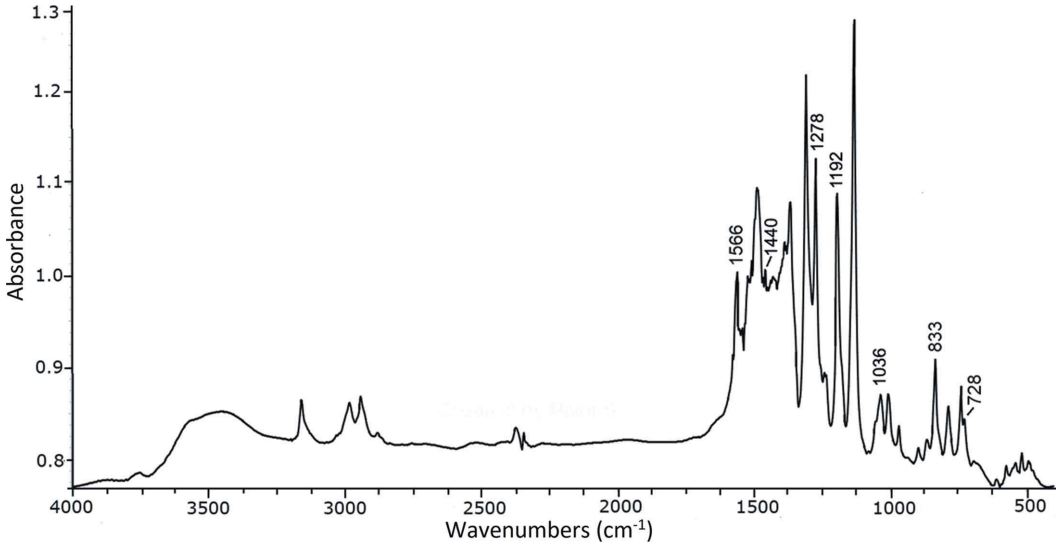

Figure 6
IR absorbance spectrum of solid-state $[Cu(NO_3)_2(tnz)_2]$.

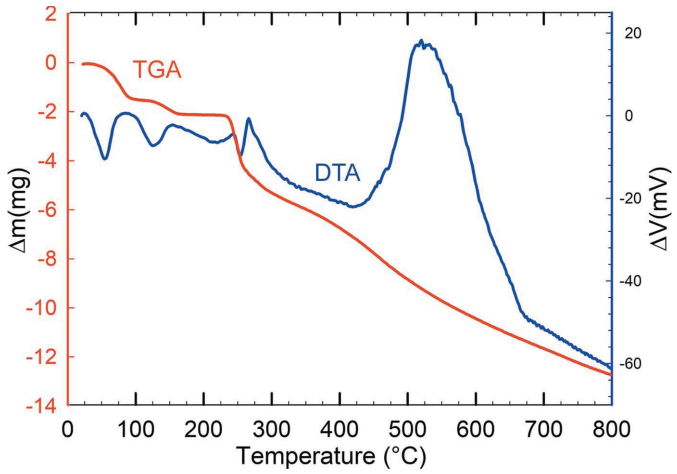

Figure 7
Thermal decomposition of $[Cu(nor)_2]SO_4{\cdot}7H_2O$.

characteristic IR bands of the tinidazole ligand are shifted compared with the uncoordinated molecule, the main changes occurring in the region of the imidazole ring vibrations. The typical ring ν(C═N) stretching mode shifts to higher frequencies (1566 cm^{-1}) relative to free tinidazole (1521 cm^{-1}), hence indicating that the ring N atom is involved in coordination to the metal. On the other hand, the asymmetric and symmetric stretching modes of the NO_2 group remain approximately at the same spectral positions, which suggests that this group is not involved in coordination, as neither is the sulfonyl group, as the band due to SO_2 stretching modes, which appears at 1192 cm^{-1} for free tinidazole, occurs at the same wavenumber in the complex.

Because the nitrate ion acts as a chelating group (see Fig. 3), strongly binding Cu^{2+} through one of its O atoms (O5) and much more weakly also by another O atom (O7), it is significantly distorted in the lattice from its ideal D_{3h} symmetry. In fact, the observed N—O bond lengths are 1.273 (3) Å for O5, 1.229 (4) Å for O7 and 1.205 (3) Å for unbonded O6. This broken symmetry is reflected in the splitting of the double-degenerate IR-active $\nu_3(E')$ mode, the absorption bands of which show up at 1440 and 1278 cm^{-1} in the IR spectrum, and also in the activation of the IR-silent $\nu_1(A_1')$ mode, which now appears as a weak band at 1036 cm^{-1}. The nitrate out-of-plane IR-active $\nu_2(A_2'')$ bending mode is assigned to the band

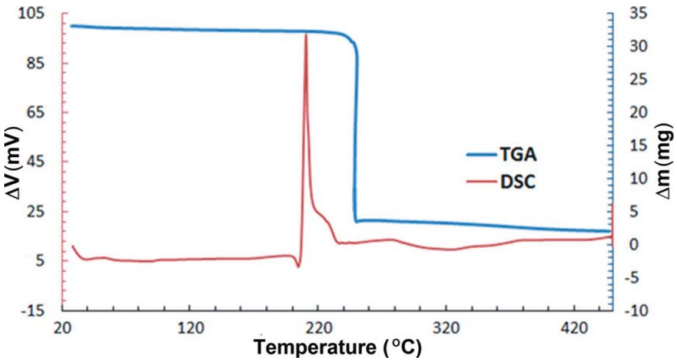

Figure 8
Thermal decomposition of $[Cu(NO_3)_2(tnz)_2]$.

observed at 833 cm^{-1} and the remaining IR-active $\nu_4(E')$ mode can be tentatively assigned to the weak feature observed at 728 cm^{-1}.

The broad band centred at about 3500 cm^{-1} is due to the stretching modes of ambient water molecules. All the above spectroscopic findings closely agree with the X-ray crystal structure results for $[Cu(NO_3)_2(tnz)_2]$ reported herein.

3.4. Thermal study

3.4.1. $[Cu(nor)_2]SO_4{\cdot}7H_2O$. The thermal behaviour of the complex is shown in Fig. 7. The TGA curve reveals that the complex decomposition starts with two well-defined weight losses in the 20–200 °C temperature range. The first corresponds to a weight loss of 11.3% (40–98 °C range) and the second to a 4.3% loss (120–166 °C range), which can be assigned to crystal dehydration. The total mass loss in this temperature interval (15.6%) compares favourably with that corresponding to the loss of the seven crystallization water molecules present in the $[Cu(nor)_2]SO_4{\cdot}7H_2O$ solid. Associated with the above weight losses, two endothermic peaks were observed at 55 and 125 °C in the DTA curve.

A continuous mass loss is observed in the TGA curve above 200 °C, accompanied by three exothermic peaks at 243, 266 and 525 °C. The exothermic peaks (DTA curve) and the irregular fall of the TGA curve suggest that various decomposition processes could occur in the temperature range 200–800 °C.

A loss of the piperazine ring (19%) is compatible with the slope change between 210 and 290 °C in the TGA curve (22%), and with the exothermic peak at 266 °C in the DTA curve.

The TGA curve in the 230–800 °C interval experiences the most significant mass loss, without well-defined steps. We speculate that two nor ligands are lost in this region with their subsequent decomposition. The final product of the heating at about 800 °C could be $CuSO_4$. The big exothermic peak observed at about 523 °C (DTA curve) could be due to by-products of the decomposition of the nor ligands (Refat, 2007). The assumptions described above are supported by the agreement between the calculated and observed mass losses. The first mass loss found up to 100 °C was 11%, in agreement with that calculated for five water molecules. The second step found (up to about 170 °C) was 4.6%, corresponding to two water molecules. The mass loss found in the region 200–800 °C was 80%, in relatively good agreement with the calculated loss of two nor ligands (70%). The final weight of the residue at 800 °C (about 17%) is in agreement with the relative mass for copper sulfate in $[Cu(nor)_2]SO_4{\cdot}7H_2O$ (17%).

Good agreement was found with a recent report on the decomposition temperatures and TGA and DTA curve profiles for a $Zn(nor)_2$ complex by Shi *et al.* (2016). In that article, it is proposed that coordination to Zn^{2+} also occurs through carbonylic and carboxylic O atoms. The temperatures and TGA–DTA curve profiles above 200 °C are similar to those observed in the present work.

3.4.2. $[Cu(NO_3)_2(tnz)_2]$. Fig. 8 shows the thermal decomposition of solid-state $[Cu(NO_3)_2(tnz)_2]$. It confirms the X-ray structure results revealing the lack of water of crystallization in the structure. TGA data show that 82.77% of the initial mass is lost in a single stage which extends up to a temperature of 250 °C. This loss is accompanied by a large exothermic DSC signal at 200 °C and is due to the partial decomposition of the complex, compatible with the formation of $CuCO_3$. One-step ligand breakdown has been reported previously by Ramachandran & Ramukutty (2015). The TGA does not show evidence of further mass losses up to about 450 °C.

4. Conclusions

Previously, when no crystals adequate for structural work were available, the sulfate salt of the copper–norfloxacin complex was described as a diaqua pentahydrate, namely, $[Cu(nor)_2(H_2O)_2]SO_4{\cdot}5H_2O$. Now our single-crystal X-ray diffraction study discloses that no water molecules bind the metal and the correct formulation is as a heptahydrate, $[Cu(nor)_2]SO_4{\cdot}7H_2O$.

Excluding the norfloxacin methyl and heterocyclic groups, the copper complex is nearly planar. The metal ion is in a square coordination (CuO_4), with two electrically neutral norfloxacin molecules acting as bidentate ligands. These ligands show in the lattice a zwitterionic charge distribution with a negatively charged $–COO^-$ group at one molecular end and a positively charged $>NH_2^+$ group at the other end.

The samples of $[Cu(NO_3)_2(tnz)_2]$ were multi-domain single crystals. This posed a challenge to find the unit-cell constants of the dominant single-crystal contributors. The problem was overcome with the assistance of PXRD data, which allowed the precise determination of the unit-cell constants. With this prior information, the detwinning software of the single-crystal diffractometer was capable of disentangling up to four contributing domains in the strongly overlapped diffraction pattern of the multi-domain sample. The structure was easily solved from the perturbed X-ray data set of one contributing domain. The $[Cu(NO_3)_2(tnz)_2]$ complex is centrosymmetric, with the Cu atom in a square environment (CuN_2O_2), *trans*-coordinated to a tinidazole N atom and a nitrate O atom.

By comparing with the spectral signature of the uncoordinated ligand, the IR spectrum of $[Cu(nor)_2]SO_4{\cdot}7H_2O$ indicates that the norfloxacin –COOH group deprotonates upon coordination to copper. Analogously, the IR spectrum of $[Cu(NO_3)_2(tnz)_2]$ shows that the tinidazole molecule acts as a monodentate ligand through its imidazole N atom. All these spectroscopic findings are in close agreement with the detailed structural X-ray data.

The TGA thermogram of $[Cu(nor)_2]SO_4{\cdot}7H_2O$ confirms the presence of the seven crystallization water molecules found in the structural X-ray diffraction study. The further decomposition of the substance proceeds as reported in the literature for this family of complexes.

The current article describes a structural, spectroscopic and thermal characterization of novel compounds with potential use as antimicrobial agents. However, additional studies are required to determine their effectiveness and possible incorporation into pharmaceutical dosage forms.

Acknowledgements

This work was supported by CONICET and UNLP of Argentina. We thank Dr J. A. Güida for help with the thermal data of $[Cu(nor)_2]SO_4{\cdot}7H_2O$. GAE and OEP are Research Fellows of CONICET.

Funding information

Funding for this research was provided by: Consejo Nacional de Investigaciones Científicas y Técnicas (grant No. PIP 0651); Universidad Nacional de La Plata (grant No. 11/X857).

References

Agilent (2011). *CrysAlis PRO*. Version 1.171.34.49. Agilent Technologies, Yarnton, Oxfordshire, England.
Alfaro-Fuentes, I., López-Sandoval, H., Mijangos, E., Duarte-Hernández, A. M., Rodriguez-López, G., Bernal-Uruchurtu, M. I., Contreras, R., Flores-Parra, A. & Barba-Behrens, N. (2014). *Polyhedron*, **67**, 373–380.
Ali, B., Tahir, S., Akhtar, M. N., Yameen, M., Ashraf, R., Hussain, T., Ghaffar, A., Abbas, M., Bokhari, T. H. & Iqbal, M. (2017). *Pol. J. Environ. Stud.* **26**, 2861–2867.
Barbas, R., Prohens, R. & Puigjaner, C. (2007). *J. Therm. Anal. Calorim.* **89**, 687–692.
Boultif, A. & Louër, D. (1991). *J. Appl. Cryst.* **24**, 987–993.
Chasseaud, L. F., Henrick, K., Matthews, R. W., Scott, P. W. & Wood, S. G. (1984). *J. Chem. Soc. Chem. Commun.* pp. 491–492.
Chongcharoen, W., Byrn, S. R. & Sutanthavibul, N. (2008). *J. Pharm. Sci.* **97**, 473–489.
Efthimiadou, E. K., Thomadaki, H., Sanakis, Y., Raptopoulou, C. P., Katsaros, N., Scorilas, A., Karaliota, A. & Psomas, G. (2007). *J. Inorg. Biochem.* **101**, 64–73.
Farrugia, L. J. (2012). *J. Appl. Cryst.* **45**, 849–854.
Laugier, J. & Bochu, B. (2000). *CHEKCELL*. Collaborative Computational Project, Number 14 (CCP14), Laboratory of Materials and Physical Engineering, School of Physics, University of Grenoble, France.
Ramachandran, E. & Ramukutty, S. (2015). *Int. J. Solid State Mater.* **1**, 1–4.
Refat, M. S. (2007). *Spectrochim. Acta A Mol. Biomol. Spectrosc.* **68**, 1393–1405.
Rigaku OD (2015). *CrysAlis PRO*. Version 1.171.38.41. Rigaku Oxford Diffraction Ltd, Yarnton, Oxfordshire, England.
Roat, R. M. (2007). In *Bioinorganic Chemistry: A Short Course*. Hoboken, New Jersey: Wiley Interscience.
Roy, S., Goud, N. R., Babu, N. J., Iqbal, J., Kruthiventi, A. K. & Nangia, A. (2008). *Cryst. Growth Des.* **8**, 4343–4346.
Ruíz, P., Ortiz, R., Perelló, L., Alzuet, G., González-Álvarez, M., Liu-González, M. & Sanz-Ruíz, F. (2007). *J. Inorg. Biochem.* **101**, 831–840.
Sánchez-Guadarrama, O., López-Sandoval, H., Sánchez-Bartéz, F., Gracia-Mora, I., Höpfl, H. & Barba-Behrens, N. (2009). *J. Inorg. Biochem.* **103**, 1204–1213.
Sekhon, B. S. & Gandhi, L. (2001). *Int. J. ChemTech Res.* **2**, 286–288.
Sheldrick, G. M. (2008). *Acta Cryst.* A**64**, 112–122.
Sheldrick, G. M. (2015*a*). *Acta Cryst.* A**71**, 3–8.
Sheldrick, G. M. (2015*b*). *Acta Cryst.* C**71**, 3–8.
Shi, Y., Chen, S., Ma, M., Wu, B., Ying, J., Xu, X. & Wang, X. (2016). *RSC Adv.* **6**, 97491–97502.
Shirley, R. (2002). In *The Crysfire 2002 system for automatic powder indexing: user's manual*. Guildford, UK: Lattice Press.
Turel, I. (2002). *Coord. Chem. Rev.* **232**, 27–47.

Visser, J. W. (1969). *J. Appl. Cryst.* **2**, 89–95.
Wallis, S. C., Gahan, L. R., Charles, B. G., Hambley, T. W. & Duckworth, P. A. (1996). *J. Inorg. Biochem.* **62**, 1–16.
Wang, G. P., Yan, L. C. & Zhu, L. G. (2003). *Chin. Chem. Lett.* **14**, 1182–1184.
Werner, P.-E., Eriksson, L. & Westdahl, M. (1985). *J. Appl. Cryst.* **18**, 367–370.
Xie, Y.-R., Ye, Q. & Xiong, R.-G. (2004). *Chin. J. Inorg. Chem.* **20**, 1007–1008.
Yvon, K., Jeitschko, W. & Parthé, E. (1977). *J. Appl. Cryst.* **10**, 73–74.